ARTICLE

High-resolution NMR structure of the antimicrobial peptide protegrin-2 in the presence of DPC micelles

K. S. Usachev · S. V. Efimov · O. A. Kolosova ·
A. V. Filippov · V. V. Klochkov

Abstract PG-1 adopts a dimeric structure in dod-ecylphosphocholine (DPC) micelles, and a channel is formed by the association of several dimers but the molecular mechanisms of the membrane damage by non-α-helical peptides are still unknown. The formation of the PG-1 dimer is important for pore formation in the lipid bilayer, since the dimer can be regarded as the primary unit for assembly into the ordered aggregates. It was supposed that only 12 residues (RGGRL-CYCRR-RFCVC-V) are needed to endow protegrin molecules with strong anti-bacterial activity and that at least four additional residues are needed to add potent antifungal properties. Thus, the 16-residue protegrin (PG-2) represents the minimal structure needed for broad-spectrum antimicrobial activity encompassing bacteria and fungi. As the peptide conformation and peptide-to-membrane binding properties are very sensitive to single amino acid substitutions, the solution structure of PG-2 in solution and in a membrane mimicking environment are crucial. In order to find evidence if the oligomerization state of PG-1 in a lipid environment will be the same or not for another protegrins, we investigate in the present work the PG-2 NMR solution structure in the presence of perdeuterated DPC micelles.

K. S. Usachev (✉) · S. V. Efimov · O. A. Kolosova ·
A. V. Filippov · V. V. Klochkov
Kazan Federal University, Kremlevskaya, 18, Kazan 420008, Russian Federation
e-mail: k.usachev@kpfu.ru

A. V. Filippov
Chemistry of Interfaces, Luleå University of Technology, 97187 Luleå, Sweden

The NMR study reported in the present work indicates that PG-2 form a well-defined structure (PDB: 2MUH) composed of a two-stranded antiparallel β-sheet when it binds to DPC micelles.

Introduction

Antimicrobial peptides (AMPs) are small peptides with a strong antibiotic activity which play an important role in the immune system of many different animals. AMPs can provide a rapid response to infection and are often effective against a broad range of bacterial species (Heller et al. 1998). The monomeric structures of small AMPs can be classified into several groups based on their amino acid compositions and structure (Brogden 2005; Friedrich et al. 2000; Jang et al. 2011; Powers and Hancock 2003; Sitaram and Nagaraj 2002; Steinberg et al. 1997; Zasloff 2002). One of them adopt an α-helical structure when bound to lipid membranes, other adopt β-type structures stabilized by disulfide bonds. These peptides adopt different structures under different conditions, allowing the conformation to adjust to the surrounding environment (Jang et al. 2006). For the disulfide-bonded β-sheet forming peptides, which includes protegrins, the presence of positively charged amino acid residues allows their strong interaction with the lipid matrix of the plasma membrane, as opposed to a protein target on the surface of the cell. Their interaction with the membrane results in permeability changes and may cause cytolysis. An AMPs cytotoxicity primarily takes place by incorporation into the membrane, ultimately disrupting its structure either by formation of pores or via

alteration of the bilayer fluidity (Brogden 2005; Gottler et al. 2008; Jang et al. 2011, 2008; Lam et al. 2006; Matsuzaki 1999; Shai 1999; Sokolov et al. 1999; Yang et al. 2000; Zasloff 2002).

Protegrins are one of the best characterized β-sheet cytolytic peptides. These small β-sheet AMPs found in porcine leukocytes (Aumelas et al. 1996; Cho et al. 1998; Fahrner et al. 1996; Kokryakov et al. 1993), are members of the cathelicidin family (Zhao et al. 1995, 1994), a large group of structurally diverse AMPs whose precursors contain a highly conserved cathelin domain (Zanetti et al. 1995). There are five known protegrins (PG-1–PG-5). The solution structure of PG-1 (PDB: 1PG1) was established by 2D NMR spectroscopy (Fahrner et al. 1996; Mani et al. 2006) and its form the β-hairpin conformation, which is composed of 18 amino acids (RGGRL-CYCRR-RFCVC-VGR) with a high content of cysteine (Cys) and positively charged arginine (Arg) residues. Six arginine residues allow PG-1 to interact with surfaces of lipid bilayers composed of negatively charged headgroups via strong electrostatic interactions.

The interaction of protegrin with the membrane depends on its lipid composition: for negatively charged anionic lipids PG-1 inserts into a membrane composed and significantly less into a membrane composed of neutrally charged lipids (Gidalevitz et al. 2003; Jang et al. 2006). It was shown that the β-forming PG-1 peptide exhibits amyloid-like ion channel behaviour in model lipid bilayers (Gottler et al. 2008; Jang et al. 2011; Sokolov et al. 1999; Yang et al. 2000) and PG-1 and Aβ share a common cellular mechanism, such as membrane disruption and pore formation, preceded by toxic ion channel formation, leading to cell death (Jang et al. 2011). PG-1 adopts a dimeric structure (PDB: 1ZY6) in dodecylphosphocholine (DPC) micelles (Aumelas et al. 1996), and a channel is formed by the association of several dimers but the molecular mechanisms of the membrane damage by non-α-helical peptides are still unknown (Bechinger 2000). It was shown that the PG-1 dimer interface of the antiparallel β-sheets in micelle environments is more stable than the parallel β-sheets and that the parallel β-sheets interact with the lipids with the β-sheet plane lying obliquely to the bilayer surface, increasing the surface pressure in the initial insertion into the lipid bilayer (Jang et al. 2007). The parallel PG-1 dimer was biologically more active to insert into the POPC lipid bilayer. The formation of the PG-1 dimer is important for pore formation in the lipid bilayer, since the dimer can be regarded as the primary unit for assembly into the ordered aggregates (Jang et al. 2007).

Study of activity of protegrins against Yeast-Phase *Candida albicans* shows that the protegrins PG-2, -3, and -5, but not PG-4, were as effective as PG-1 (Cho et al. 1998). These studies suggest that only 12 residues are needed to endow protegrin molecules with strong antibacterial activity and that at least 4 additional residues are needed to add potent antifungal properties. Thus, the 16-residue protegrin PG-2 likely represents the minimal structure needed for broad-spectrum antimicrobial activity encompassing bacteria and fungi (Cho et al. 1998). As the peptide conformation and peptide-to-membrane binding properties are very sensitive to single amino acid substitutions (Usachev et al. 2014), the solution structure of PG-2, -3, -4, and -5 in solution and in a membrane mimicking environment are crucial. In order to find evidence if the oligomerization state of PG-1 in a lipid environment will be the same for another protegrins, we investigate in the present work the PG-2 NMR solution structure in the presence of perdeuterated DPC micelles which is a commonly used zwitterionic detergent for the solubilization of membrane peptides and proteins (McDonnell and Opella 1993; Roumestand et al. 1998). Here we should mentioned that even though solution NMR experiments on DPC micelles provide high-resolution structures, the structural results obtained from a detergent micelle need to be substantiated by studies in lipid bilayers, which do not have a curved surface and are a better approximation to cell membranes. Contrariwise for some AMPs such as magainins MSI-594 and MSI-78 was observed that the formation of antiparallel dimers and magainin aggregation is driven by the primary sequence rather than the membrane mimicking system (i.e., detergent micelles vs. lipid vesicles) (Porcelli et al. 2006). Also the solution NMR in micelles offers as compared to the vesicles the higher sensitivity.

Materials and methods

Sample preparation

The PG-2 peptides were synthesized by Dr. Andrey Filippov in Chemistry of Interfaces laboratory at the Luleå University of Technology. Peptides were synthesized by solid-phase peptide synthesis, using amino acids protected by the 9-fluorenylmethoxycarbonyl group and with reaction mixture conductivity control. Fmoc-protected amino acids of "peptide synthesis" grade were purchased from Applied Biosystems, Foster City, CA, USA. Peptide synthesis was done using the 0.1 mmol automated fast Fmoc solid phase procedure using HBTU (H-benzotriazole-1-yl-tetramethyluranium hexafluorophosphate) activation. The procedure was performed on an ABI 433A peptide synthesizer (Applied Biosystems) at 293 K. Cleavage from the resin and separation of the peptide substrate and the protecting groups was carried out in a solution of phenol, ethanedithiol and thioanisole in 95 % trifluoroacetic acid, followed by precipitation of the peptide in cold tert-butyl

methyl ether (tBME). The peptide was purified using the high-performance liquid chromatography instrument Series 200 Perkin–Elmer HPLC System (Waltham, MA, USA). A semipreparative Vydac 259VH810 reverse phase column was used at 328 K, with a water-acetonitrile linear gradient with 0.1 % trifluoroacetic acid (TFA) and flow rate of 4 mL/min. The quality of the final product was characterized using electrospray mass spectrometry. The purity of the peptide was estimated as better than 95 %. The sample was lyophilized and stored at a temperature of 193 K before use.

The NMR samples of PG-2 were prepared as previously described for PG-1 (Roumestand et al. 1998). The peptide (4 mg) was solubilized in an aqueous solution (H_2O or ^2H_2O, 500 µL) containing 20 mg perdeuterated DPC (molar ratio ∼ 1:12). 3-(trimethylsilyl)-propionic-2,2,3,3-$^2H_4$ acid (TMSP-2,2,3,3-$^2H_4$) (98 % atom ^2H, Aldrich) was added as an internal chemical shift standard for ^1H NMR spectroscopy. Perdeuterated d_{38} DPC (98 % ^2H) and TSP-d_4 were purchased from Aldrich.

NMR spectroscopy and spatial structure calculation

All data were acquired at 500 MHz (Bruker Avance II) NMR spectrometer at a probe temperature 293 K. The proton chemical shifts were referred to the TMSP-2,2,3,3-$^2H_4$. 2D NOESY, TOCSY and DIPSY experiments were reordered in the phase-sensitive state-TPPI mode. The spin-lock time of the TOCSY and DIPSI was 60, 100 and 130 ms. Solvent suppression was carried out using the "3-9-19" pulse sequence with gradients using flip-back pulse in NOESY experiments (Lippens et al. 1995; Piotto et al. 1992; Sklenar et al. 1993); using excitation sculpting with gradients in DIPSI experiments (Hwang and Shaka 1995; Shaka et al. 1988) and using watergate W5 pulse sequence with gradients in TOCSY experiments (Bax and Davis 1985; Liu et al. 1998). NOESY data were collected with a mixing time of 200, 300 and 500 ms to derive ^1H–^1H distance constraints. A total of 32 (TOCSY and DIPSI) or 64 (NOESY) transient were acquired. All 2D spectra were recorded with 512 × 4,096 data points and with a spectral width of 6,000 Hz.

Spectra were processed by NMRPipe (Delaglio et al. 1995) and analyzed using SPARKY. Sequence-specific backbone resonance assignments and side-chain assignments for all residues were obtained using a combination of 2D TOCSY, DIPSI and NOESY experiments.

Inter-proton distances obtained from analysis of intensities of cross-peaks from NMR NOESY spectra were used as the primary data for the calculations by the molecular dynamics method. Following structural calculations, the ensemble of structures was subjected to restrained molecular dynamics using the Xplor-NIH (Schwieters et al.

2003). A total of 1,000 structures were calculated and 20 with minimal energy were chosen. None of the 20 structures had any violated NOE distances. Individual structures were minimized, heated to 1,000 K for 6,000 steps, cooled in 100 K increments to 50 K, each with 3,000 steps, and finally minimized with 1,000 steps of the steepest descent, followed by 1,000 steps of conjugate gradient minimization. Starting with a family of 1,000 structures, approximately 200 were subjected to subsequent molecular dynamics calculations and, finally, the 20 lowest energy structures were retained. Ramachandran plot and structure validation was made with MolProbity (Chen et al. 2010; Davis et al. 2007). The most probable structure of the "peptide-micelle" complex was determined by binding the hydrophobic area of the peptide on the charged micelle surface. The PG-2 peptide structures were visualized with MOLMOL (Koradi et al. 1996) and CHIMERA (Pettersen et al. 2004).

Results and discussion

Chemical shift assignments of PG-2 in DPC micelles were obtained using standard methods of protein NMR spectroscopy by 2D NMR ^1H–^1H TOCSY and NOESY experiments (Table 1). Chemical shifts were deposited in the BioMagResBank (BMRB ID 25212). Figure 1 shows the ^1H–^1H NMR NOESY spectra of PG-2 at 293 K in H_2O solution and in the presence of DPC at a detergent/protein

Table 1 Proton chemical shifts in ppm measured in water for PG-2 in the presence of perdeuterated DPC micelles (detergent/peptide molar ratio ∼ 12) at 293 K

Residue	Chemical shift (ppm)					
	NH	α	β	γ	δ	ε
R1	–	4.08	1.92	1.67	3.19	7.40
G2	8.95	4.00	–	–	–	–
G3	8.33	3.86	–	–	–	–
R4	8.28	4.38	1.74	1.60	3.11	7.27
L5	8.48	4.55	1.74	1.58	0.90	–
C6	8.30	5.70	2.85, 2.66	–	–	–
Y7	8.19	4.67	2.84	–	7.00	6.69
C8	9.15	5.69	2.86, 2.66	–	–	–
R9	9.23	4.35	1.85	1.61	3.30	7.76
R10	9.24	3.77	2.05	1.66	3.28	7.61
R11	8.12	3.97	2.03, 1.86	1.37	3.10	7.26
F12	8.48	3.86	2.94, 2.68	–	–	–
C13	8.81	5.67	2.95, 2.69	–	–	–
V14	8.95	4.38	2.04	1.01	–	–
C15	8.86	5.57	2.86, 2.66	–	–	–
V16	8.81	4.34	2.24	0.95	–	–

ratio of ∼ 12. Chemical shift deviation relative to random coil values (Wishart et al. 1992) of PG-2 in the presence of DPC were found to be the similar with PG-1 (Fig. 2) (Roumestand et al. 1998). Two "dense" group of three or more downfield shifts indicate on the presence of β-strand
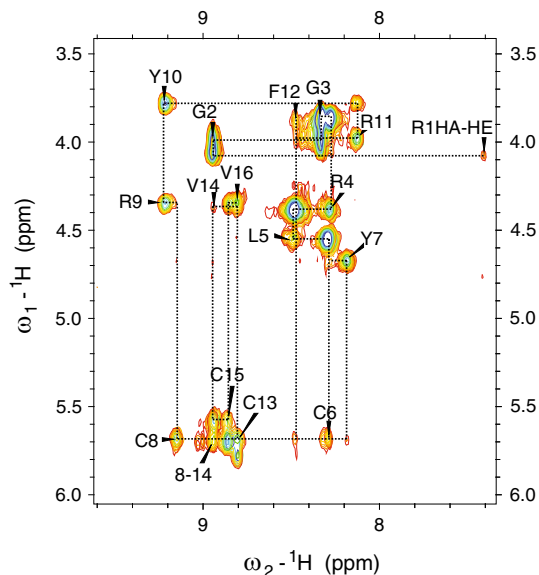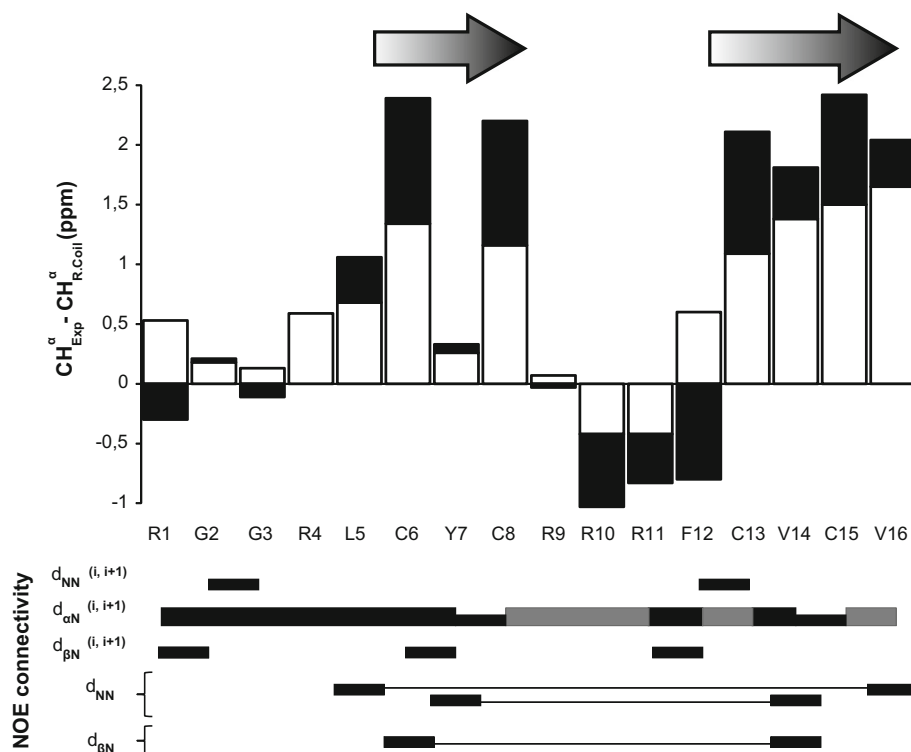

Fig. 1 Fingerprint NH-Hα region of a 2D NMR ^{1}H–^{1}H NOESY spectrum acquired at 500 MHz of PG-2 in a solution of $H_2O + D_2O$ with DPC micelles. Mixing time $t_m = 0.15$ s

structure. Furthermore the presence of $dNN_{(i,i+1)}$ and $d\alpha N_{(i,i+1)}$ medium range NOE connectivities (Fig. 2) in 2D NOESY NMR spectra of PG-2 in DPC micelles also is an indication of partially folded structure suggest that the PG-2 adopts a β-hairpin in the regions of 6–9 and 12–15 residues. A total of 174 interproton NOE distance constraints were determined for the structural calculations (see Table 2). Numerous medium-range NOE connectivities allowed us to construct the 3D structure of PG-2 in the presence of DPC micelles by molecular dynamics method calculations of the Xplor-NIH program (Schwieters et al. 2003). The 20 lowest-energy structures of PG-2 were used for the final analysis. The final NMR ensemble of 20 structures has been deposited in the Protein Data Bank (PDB: 2MUH). Ramachandran analysis for 20 structures of PG-2 in the precence of DPC micelles shown in Fig. 3. 78.6 % of all residues were in favored (98 %) regions and 100.0 % of all residues were in allowed (>99.8 %) regions.

Stereo views of a superposition of this family of structures are shown in Fig. 4. Most of the structure is well defined with a an overall backbone root mean squared deviation (RMSD) of 1.33 Å. As expected from the chemical shift deviations and NOE crosspeak patterns, PG-2 forms an anti-parallel β sheet from residues 6–9 and 12–15. Likewise for the PG-1 we observed that for PG-2 the sidechains of Leu5, Phe12, Val14 and Val16 forms a relatively well ordered apolar cluster (Aumelas et al. 1996; Fahrner et al. 1996) (Fig. 4). Based on these data we

Fig. 2 Summary of the chemical shift deviations of α-proton resonances relative to random coil values in water (Wishart et al. 1992) and NOE connectivity. *Open bars* are for PG-2 and *filled bars* for PG-1 (Roumestand et al. 1998) in the precence of DPC micelles (detergent/peptide ratio ∼2). *The line thickness* for the NOE connectivity is inversely proportional to the squared upper distance bound. When an unambiguous assignment was not possible due to peak overlap, the NOEs are drawn with *gray shaded boxes*
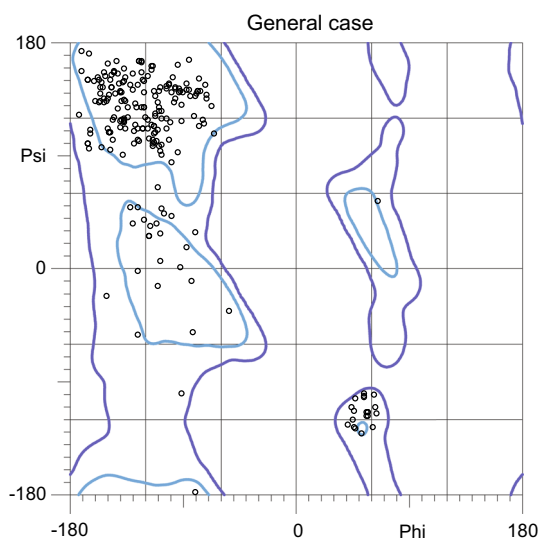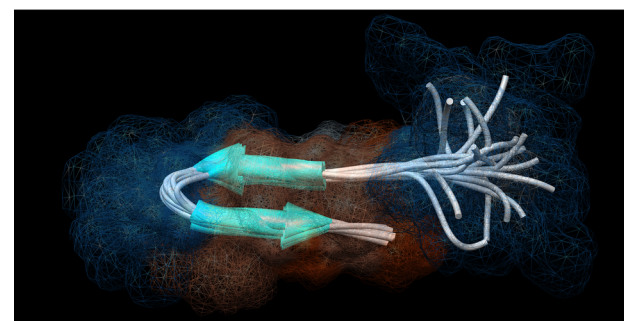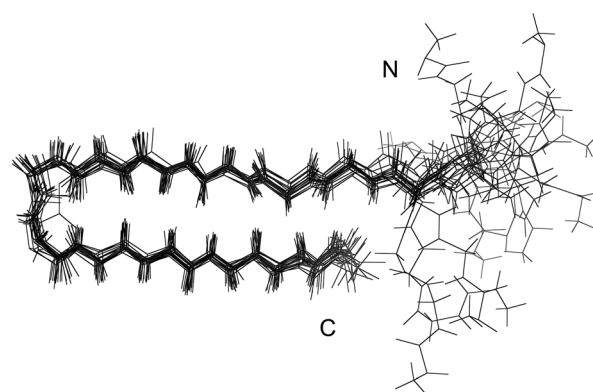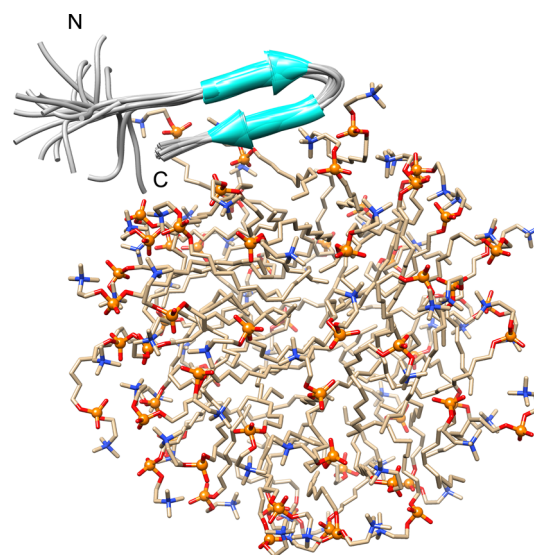
Table 2 Structural statistics for the 20 best NMR structures of PG-2 in a solution of $H_2O + D_2O$ with DPC micelles

Distance restraints used for structure calculation	Total
Interproton restraints	174
Intraresidue	127
Sequential ($|i - j| = 1$)	28
Medium-range ($1 < |i - j| \leq 4$)	8
Long-range ($|i - j| > 4$)	11

Fig. 3 Ramachandran analysis for 20 structures of PG-2 in the precence of DPC micelles. 78.6 % of all residues were in favored (98 %) regions and 100.0 % of all residues were in allowed (>99.8 %) regions

Fig. 4 The superposition of 20 minimized structures for the PG-2 (2MUH) in a solution of $H_2O + D_2O$ with DPC micelles. Only backbone atoms shown as sticks at the *top* and ribbon and hydrophobicity surface (as transparent mesh) of the PG-2 are shown at the *bottom*

Fig. 5 Proposed structure for PG-2 bound to a DPC micelle

hypothesize that PG-2 interact with the DPC micelle by binding the hydrophobic area of the peptide on the charged micelle surface (Blochin et al. 2013; Blokhin et al. 2014; Usachev et al. 2013a, b). These observations also supports the hypothesis of the requirement of hydrophobic/hydrophilic cluster proximity to induce cytolytic activity of protegrins (Aumelas et al. 1996). The final structure of the PG-2 peptide bound to an SDS micelle is presented in Fig. 5. Comparing the obtained backbone structure of PG-2 in DPC micelles with solved previously PG-1 structure in solution (PDB: 1PG1) we could conclude that both structures are quite similar (Fig. 6). The differences are observed for residues closed to disulfide bond bonds (Tyr7, Cys8, Cys13) and in the loop region (Arg9, Arg11, Cys13) and for the residues of apolar cluster (Leu5, Phe12, Val14 and Val16) the differences in backbone structure were minimal.

Several studies of the PG-1 and its analogues interaction with lipid bilayers showed that there are a membrane thinning effect, ability of pore formation and that PG-1 can adopt a dimer (Jang et al. 2006, 2007; Khandelia and Kaznessis 2007; Rodziewicz-Motowidlo et al. 2010; Roumestand et al. 1998). PG-2 is identical to PG-1 except for its deletion of residues 17 and 18 (Gly-Arg). Was shown that each region of the PG molecule, with the exception of

Fig. 6 90-degree-rotated stereo views of a superposition of PG-1 (*green*; PDB: 1PG1) and PG-2 (*magneta*; PDB: 2MUH) structures. The differences are observed for residues closed to disulfide bond bonds (Tyr7, Cys8, Cys13) and in the loop region (Arg9, Arg11, Cys13). The progression of views rotates 90° about a horizontal axis (for the color interpretation the reader is referred to the web version of this paper)
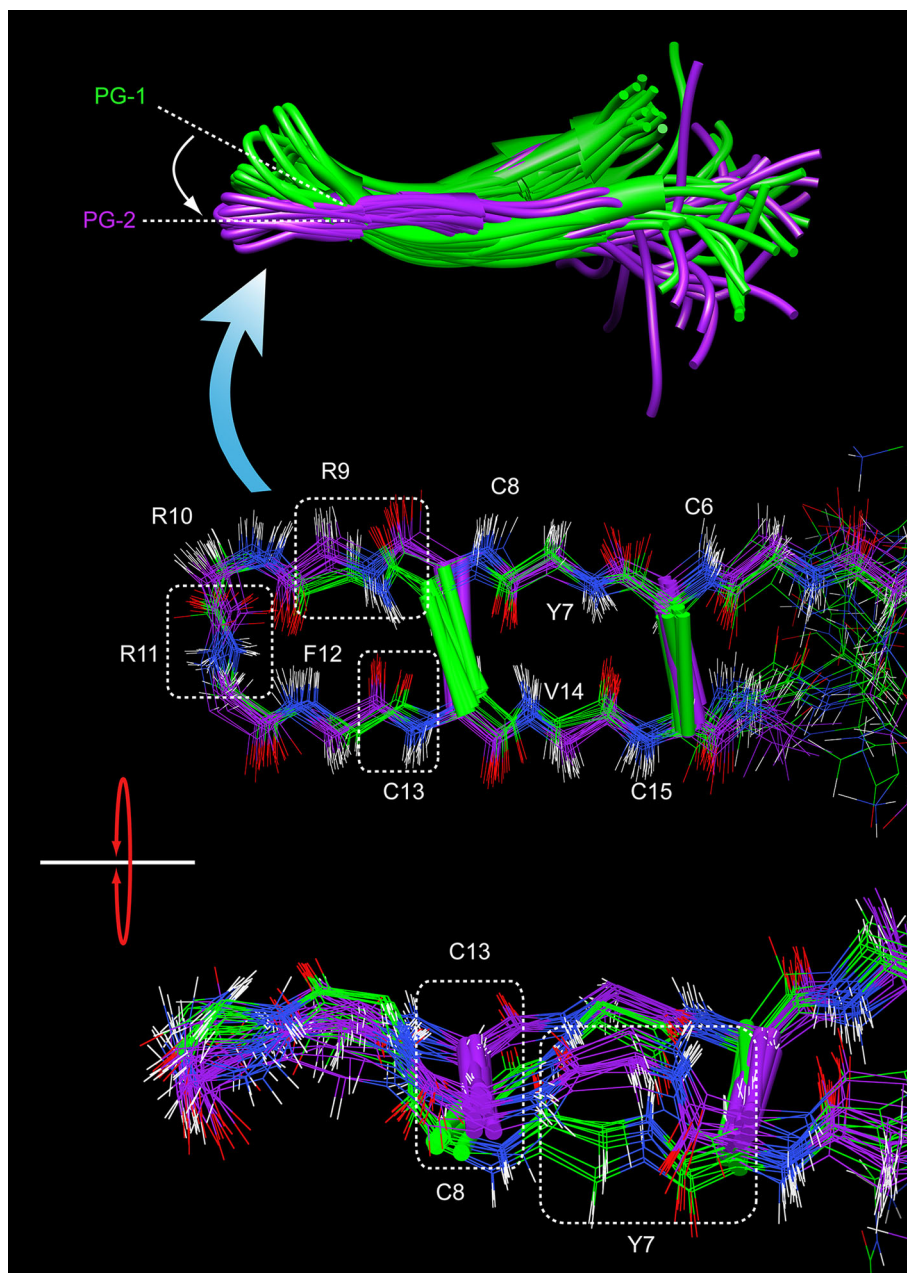
residues 17 and 18, contributed substantially to activity against *C. albicans* (Cho et al. 1998). In contrast, only 12 residues (residues 5–16) and their two associated disulfide bonds sufficed to endow PG-1 with strong antibacterial properties and, the 16-residue protegrin PG-2 may already approach the minimal structure that is capable of exerting strong activity against gram-positive bacteria, gram-negative bacteria, and fungi in an extracellular environment.

In contrast with PG-1, for PG-2 in the presence of DPC micelles there were not inconsistent with β-sheet structure NOEs (Roumestand et al. 1998). For PG-1 in DPC micelles a strong $d_{\alpha\alpha}$ NOE effects observed between residues R18

and F12, V14 and V16. These "inconsistent" NOEs appears due to formation of an additional antiparallel β-sheet between two monomers. But in PG-2 sequence there are no G17 and V18 residues, so only interaction between V14 and V16 residues is possible. We recorded 2D ^{1}H–^{1}H NMR NOESY spectra of PG-2 in the presence of DPC micelles in ^{2}H$_2$O and didn't observe a $d_{\alpha\alpha}$ NOE effect between V14 and V16. Partially this may be due to the close values of the V14 and V16 CH$^\alpha$ chemical shifts. Nevertheless the dimeric structure by PG-2 in a lipid environment can take place due to its antimicrobial activity similarly as for PG-1 or for the human defensin HNP-3

(Hill et al. 1991). This this assumption can be proved by other methods for example by Rotational-Echo Double-Resonance Solid-State NMR as it was shown for PG-1 (Mani et al. 2006).

Conclusion

In this article, we report the conformation of the PG-2 antimicrobial peptide in the presence of DPC micelles studied by 2D NMR spectroscopy. The NMR study reported in the present work indicates that PG-2 form a well-defined structure (2MUH) composed of a two-stranded antiparallel β-sheet when it binds to DPC micelles. Likewise for the PG-1 we observed that for PG-2 the sidechains of Leu5, Phe12, Val14 and Val16 forms a relatively well ordered apolar cluster and based on these data we hypothesize that PG-2 interact with the DPC micelle by binding the hydrophobic area of the peptide on the charged micelle surface. In contrast with PG-1, for PG-2 in presence of DPC micelles, no intramolecular NOEs were observed. Partially this may be due to the close values of the V14 and V16 CH^α chemical shifts. Nevertheless the dimeric structure by PG-2 in a lipid environment can take place due to its antimicrobial activity similarly as for PG-1 or for the human defensin HNP-3. However, this hypothesis requires more experimental studies.

References

Aumelas A, Mangoni M, Roumestand C, Chiche L, Despaux E, Grassy G, Calas B, Chavanieu A (1996) Synthesis and solution structure of the antimicrobial peptide protegrin-1. Eur J Biochem 237:575–583. doi:10.1111/j.1432-1033.1996.0575p.x

Bax A, Davis DG (1985) Mlev-17-based two-dimensional homonuclear magnetization transfer spectroscopy. J Magn Reson 65:355–360. doi:10.1016/0022-2364(85)90018-6

Bechinger B (2000) Understanding peptide interactions with the lipid bilayer: a guide to membrane protein engineering. Curr Opin Chem Biol 4:639–644. doi:10.1016/S1367-5931(00)00143-5

Blochin DS, Aganova OV, Yulmetov AR, Filippov A, Gizatulin BL, Afonin S, Klochkov VV (2013) Spatial structure of heptapeptide Glu-Ile-Leu-Asn-His-Met-Lys, a fragment of the HIV enhancer prostatic acid phosphatase, in aqueous and SDS micelle solutions. J Mol Struct 1033:59–66. doi:10.1016/j.molstruc.2012.08.018

Blokhin DS, Filippov AV, Antzutkin ON, Karataeva FK, Klochkov VV (2014) Spatial structure of oligopeptide PAP(248–261), the N-terminal fragment of the HIV enhancer prostatic acid phosphatase peptide PAP(248–286), in aqueous and SDS micelle

solutions. J Mol Struct 1070:38–42. doi:10.1016/j.molstruc.2014.04.019

Brogden KA (2005) Antimicrobial peptides: pore formers or metabolic inhibitors in bacteria? Nat Rev Microbiol 3:238–250. doi:10.1038/Nrmicro1098

Chen VB, Arendall WB 3rd, Headd JJ, Keedy DA, Immormino RM, Kapral GJ, Murray LW, Richardson JS, Richardson DC (2010) Molprobity: all-atom structure validation for macromolecular crystallography. Acta Crystallogr D 66:12–21. doi:10.1107/S0907444909042073

Cho Y, Turner JS, Dinh NN, Lehrer RI (1998) Activity of protegrins against yeast-phase *Candida albicans*. Infect Immun 66:2486–2493

Davis IW, Leaver-Fay A, Chen VB, Block JN, Kapral GJ, Wang X, Murray LW, Arendall WB III, Snoeyink J, Richardson JS, Richardson DC (2007) Molprobity: all-atom contacts and structure validation for proteins and nucleic acids. Nucleic Acids Res 35:W375–W383. doi:10.1093/Nar/Gkm216

Delaglio F, Grzesiek S, Vuister GW, Zhu G, Pfeifer J, Bax A (1995) NMRpipe—a multidimensional spectral processing system based on unix pipes. J Biomol NMR 6:277–293. doi:10.1007/Bf00197809

Fahrner RL, Dieckmann T, Harwig SSL, Lehrer RI, Eisenberg D, Feigon J (1996) Solution structure of protegrin-1, a broad-spectrum antimicrobial peptide from porcine leukocytes. Chem Biol 3:543–550. doi:10.1016/S1074-5521(96)90145-3

Friedrich CL, Moyles D, Beveridge TJ, Hancock REW (2000) Antibacterial action of structurally diverse cationic peptides on gram-positive bacteria. Antimicrob Agents Chemother 44:2086–2092. doi:10.1128/Aac.44.8.2086-2092.2000

Gidalevitz D, Ishitsuka YJ, Muresan AS, Konovalov O, Waring AJ, Lehrer RI, Lee KYC (2003) Interaction of antimicrobial peptide protegrin with biomembranes. Proc Natl Acad Sci U S A 100:6302–6307. doi:10.1073/pnas.0934731100

Gottler LM, Bea RD, Shelburne CE, Ramamoorthy A, Marsh ENG (2008) Using fluorous amino acids to probe the effects of changing hydrophobicity on the physical and biological properties of the beta-hairpin antimicrobial peptide protegrin-1. Biochemistry 47:9243–9250. doi:10.1021/Bi801045n

Heller WT, Waring AJ, Lehrer RI, Huang HW (1998) Multiple states of beta-sheet peptide protegrin in lipid bilayers. Biochemistry 37:17331–17338. doi:10.1021/Bi981314q

Hill CP, Yee J, Selsted ME, Eisenberg D (1991) Crystal-structure of defensin Hnp-3, an amphiphilic dimer—mechanisms of membrane permeabilization. Science 251:1481–1485. doi:10.1126/science.2006422

Hwang TL, Shaka AJ (1995) Water suppression that works—excitation sculpting using arbitrary wave-forms and pulsed-field gradients. J Magn Reson Ser A 112:275–279. doi:10.1006/jmra.1995.1047

Jang H, Ma B, Woolf TB, Nussinov R (2006) Interaction of protegrin-1 with lipid bilayers: membrane thinning effect. Biophys J 91:2848–2859. doi:10.1529/biophysj.106.084046

Jang H, Ma BY, Nussinov R (2007) Conformational study of the protegrin-I (PG-I) dimer interaction with lipid bilayers and its effect. BMC Struct Biol. doi:10.1186/1472-6807-7-21

Jang H, Ma B, Lal R, Nussinov R (2008) Models of toxic beta-sheet channels of protegrin-1 suggest a common subunit organization motif shared with toxic alzheimer beta-amyloid ion channels. Biophys J 95:4631–4642. doi:10.1529/biophysj.108.134551

Jang H, Arce FT, Mustata M, Ramachandran S, Capone R, Nussinov R, Lal R (2011) Antimicrobial protegrin-1 forms amyloid-like fibrils with rapid kinetics suggesting a functional link. Biophys J 100:1775–1783. doi:10.1016/j.bpj.2011.01.072

Khandelia H, Kaznessis YN (2007) Structure of the antimicrobial beta-hairpin peptide protegrin-1 in a DLPC lipid bilayer investigated

by molecular dynamics simulation. BBA-Biomembr 1768:509–520. doi:10.1016/j.bbamem.2006.11.015

Kokryakov VN, Harwig SSL, Panyutich EA, Shevchenko AA, Aleshina GM, Shamova OV, Korneva HA, Lehrer RI (1993) Protegrins—leukocyte antimicrobial peptides that combine features of corticostatic defensins and tachyplesins. FEBS Lett 327:231–236. doi:10.1016/0014-5793(93)80175-T

Koradi R, Billeter M, Wuthrich K (1996) MOLMOL: a program for display and analysis of macromolecular structures. J Mol Gr 14:51–55. doi:10.1016/0263-7855(96)00009-4

Lam KLH, Ishitsuka Y, Cheng YS, Chien K, Waring AJ, Lehrer RI, Lee KYC (2006) Mechanism of supported membrane disruption by antimicrobial peptide protegrin-1. J Phys Chem B 110:21282–21286. doi:10.1021/Jp0630065

Lippens G, Dhalluin C, Wieruszeski JM (1995) Use of a water flip-back pulse in the homonuclear noesy experiment. J Biomol NMR 5:327–331

Liu ML, Mao XA, Ye CH, Huang H, Nicholson JK, Lindon JC (1998) Improved WATERGATE pulse sequences for solvent suppression in NMR spectroscopy. J Magn Reson 132:125–129. doi:10.1006/jmre.1998.1405

Mani R, Tang M, Wu X, Buffy JJ, Waring AJ, Sherman MA, Hong M (2006) Membrane-bound dimer structure of a beta-hairpin antimicrobial peptide from rotational-echo double-resonance solid-state NMR. Biochemistry 45:8341–8349. doi:10.1021/Bi060305b

Matsuzaki K (1999) Why and how are peptide–lipid interactions utilized for self-defense? magainins and tachyplesins as archetypes. BBA-Biomembr 1462:1–10. doi:10.1016/S0005-2736(99)00197-2

McDonnell PA, Opella SJ (1993) Effect of detergent concentration on multidimensional solution NMR-spectra of membrane-proteins in micelles. J Magn Reson Ser B 102:120–125. doi:10.1006/jmrb.1993.1073

Pettersen EF, Goddard TD, Huang CC, Couch GS, Greenblatt DM, Meng EC, Ferrin TE (2004) UCSF chimera—a visualization system for exploratory research and analysis. J Comput Chem 25:1605–1612. doi:10.1002/Jcc.20084

Piotto M, Saudek V, Sklenar V (1992) Gradient-tailored excitation for single-quantum NMR-spectroscopy of aqueous-solutions. J Biomol NMR 2:661–665. doi:10.1007/Bf02192855

Porcelli F, Buck-Koehntop BA, Thennarasu S, Ramamoorthy A, Veglia G (2006) Structures of the dimeric and monomeric variants of magainin antimicrobial peptides (MSI-78 and MSI-594) in micelles and bilayers, determined by NMR spectroscopy. Biochemistry 45:5793–5799. doi:10.1021/bi0601813

Powers JPS, Hancock REW (2003) The relationship between peptide structure and antibacterial activity. Peptides 24:1681–1691. doi:10.1016/j.peptides.2003.08.023

Rodziewicz-Motowidlo S, Mickiewicz B, Greber K, Sikorska E, Szultka L, Kamysz E, Kamysz W (2010) Antimicrobial and conformational studies of the active and inactive analogues of the protegrin-1 peptide. FEBS J 277:1010–1022. doi:10.1111/j.1742-4658.2009.07544.x

Roumestand C, Louis V, Aumelas A, Grassy G, Calas B, Chavanieu A (1998) Oligomerization of protegrin-1 in the presence of DPC micelles. A proton high-resolution NMR study. FEBS Lett 421:263–267. doi:10.1016/S0014-5793(97)01579-2

Schwieters CD, Kuszewski JJ, Tjandra N, Clore GM (2003) The Xplor-NIH NMR molecular structure determination package. J Magn Reson 160:65–73. doi:10.1016/S1090-7807(02)00014-9

Shai Y (1999) Mechanism of the binding, insertion and destabilization of phospholipid bilayer membranes by alpha-helical antimicrobial and cell non-selective membrane-lytic peptides. BBA-Biomembr 1462:55–70. doi:10.1016/S0005-2736(99)00200-X

Shaka AJ, Lee CJ, Pines A (1988) Iterative schemes for bilinear operators—application to spin decoupling. J Magn Reson 77:274–293. doi:10.1016/0022-2364(88)90178-3

Sitaram N, Nagaraj R (2002) Host-defense antimicrobial peptides: importance of structure for activity. Curr Pharm Design 8:727–742. doi:10.2174/1381612023395358

Sklenar V, Piotto M, Leppik R, Saudek V (1993) Gradient-tailored water suppression for H-1-N-15 Hsqc experiments optimized to retain full sensitivity. J Magn Reson Ser A 102:241–245. doi:10.1006/jmra.1993.1098

Sokolov Y, Mirzabekov T, Martin DW, Lehrer RI, Kagan BL (1999) Membrane channel formation by antimicrobial protegrins. BBA-Biomembr 1420:23–29. doi:10.1016/S0005-2736(99)00086-3

Steinberg DA et al (1997) Protegrin-1: a broad-spectrum, rapidly microbicidal peptide with in vivo activity. Antimicrob Agents Chemother 41:1738–1742

Usachev KS, Filippov AV, Antzutkin ON, Klochkov VV (2013a) Use of a combination of the RDC method and NOESY NMR spectroscopy to determine the structure of Alzheimer's amyloid A beta(10–35) peptide in solution and in SDS micelles. Eur Biophys J 42:803–810. doi:10.1007/s00249-013-0928-7

Usachev KS, Filippov AV, Filippova EA, Antzutkin ON, Klochkov VV (2013b) Solution structures of Alzheimer's amyloid A beta(13–23) peptide: NMR studies in solution and in SDS. J Mol Struct 1049:436–440. doi:10.1016/j.molstruc.2013.06.043

Usachev KS, Filippov AV, Khairutdinov BI, Antzutkin ON, Klochkov VV (2014) NMR structure of the arctic mutation of the alzheimer's Aβ(1–40) peptide docked to SDS micelles. J Mol Struct 1076:518–523. doi:10.1016/j.molstruc.2014.08.030

Wishart DS, Sykes BD, Richards FM (1992) The Chemical-shift index—a fast and simple method for the assignment of protein secondary structure through NMR-spectroscopy. Biochemistry 31:1647–1651. doi:10.1021/Bi00121a010

Yang L, Weiss TM, Lehrer RI, Huang HW (2000) Crystallization of antimicrobial pores in membranes: magainin and protegrin. Biophys J 79:2002–2009

Zanetti M, Gennaro R, Romeo D (1995) Cathelicidins—a novel protein family with a common proregion and a variable C-terminal antimicrobial domain. FEBS Lett 374:1–5. doi:10.1016/0014-5793(95)01050-O

Zasloff M (2002) Antimicrobial peptides of multicellular organisms. Nature 415:389–395. doi:10.1038/415389a

Zhao CQ, Liu LD, Lehrer RI (1994) Identification of a new member of the protegrin family by cDNA cloning. FEBS Lett 346:285–288. doi:10.1016/0014-5793(94)00493-5

Zhao CQ, Ganz T, Lehrer RI (1995) The structure of porcine protegrin genes. FEBS Lett 368:197–202. doi:10.1016/0014-5793(95)00633-K